Semina Ciências Exatas e Tecnológicas

e-ISSN 1679-0375
ARCHAEOMETRY

ORIGINAL ARTICLE DOI 10.5433/1679-0375.2025.v46.52708

iThenticate

Evaluation of Artifacts Produced by a Commercial Portable XRF Device and their Influence on the Analysis of Artworks

Avaliação dos Artefatos Gerados por um Dispositivo Portátil de XRF Comercial e sua Influência na Análise de Obras de Arte

Roberta Manon de Paula Sales Borges[1], Josiane Emerich Cavalcante[1], Isis Verona Nascimento da Silva Franzi[2], Anderson Gomes de Paula[2], Evelyne Azevedo[3], Ricardo Tadeu Lopes[4], Davi Ferreira de Oliveira[4]

Received: April 3, 2025 *Received in revised form: June 25, 2025* *Accepted: July 15, 2025* *Available online: July 31, 2025*

ABSTRACT

This study investigates the origin and impact of spectral interferences associated with the Bruker Tracer III portable X-ray fluorescence (pXRF) spectrometer, used by the authors for elemental characterization of cultural heritage objects. Systematic analyses were conducted on reference materials and on the sculpture *Head of Apollo* from the Eva Klabin House Museum, Rio de Janeiro, facilitating the detection of instrumental peaks and improving the accuracy of qualitative analyses by minimizing instrument-derived interferences. Measurements were carried out under controlled conditions, both with and without the spectrometer's radiation protection shield, using fixed operational parameters (40 kV, 35 μA and 60 s). The resulting spectra revealed peaks attributable to the instrument's structural components. With the shield in place, elements such as Ca, Ti, Fe, Ni, Cu, Zn, and Pb were detected. In the absence of the shield, the peaks corresponding to Ca, Zn, and Pb were suppressed, although interferences from the remaining elements persisted.

keywords portable X-ray fluorescence, instrumental characterization, spectral interferences, archaeometry

RESUMO

Este estudo investiga a origem e o impacto das interferências espectrais associadas ao espectrômetro portátil de fluorescência de raios X (pXRF) Bruker Tracer III, utilizado pelos autores na caracterização elementar de objetos do patrimônio cultural. Foram realizadas análises sistemáticas em materiais de referência e na escultura Cabeça de Apolo da Casa Museu Eva Klabin, Rio de Janeiro, permitindo a identificação de picos instrumentais e aprimorando a precisão das análises qualitativas pela minimização das interferências derivadas do instrumento. As medições foram realizadas em condições controladas, com e sem o escudo de proteção contra radiação do espectrômetro, utilizando parâmetros operacionais fixos (40 kV, 35 μA e 60 s). Os espectros resultantes revelaram picos atribuíveis aos componentes estruturais do instrumento. Com o escudo em posição, foram detectados elementos como Ca, Ti, Fe, Ni, Cu, Zn e Pb. Na ausência do escudo, os picos correspondentes a Ca, Zn e Pb foram suprimidos, embora as interferências dos demais elementos tenham persistido.

palavras-chave fluorescência de raios X portátil, caracterização instrumental, interferências espectrais, arqueometria

[1]PhD Student, Nuclear Engineering Program - NEP/UFRJ, Rio de Janeiro, RJ, Brazil. robertamanon2009@gmail.com, emerichcavalcante@hotmail.com
[2]Postdoctoral Researcher, NEP/UFRJ, Rio de Janeiro, RJ, Brazil. isisfranzi@gmail.com, eng.agp@gmail.com
[3]Prof. Dr., Arts Institute, UERJ, Rio de Janeiro, RJ, Brazil. evelyneazevedo@gmail.com
[4]Prof. Dr., NEP/UFRJ, Rio de Janeiro, RJ, Brazil. rlopes@coppe.ufrj.br, davifoliveira@coppe.ufrj.br

Introduction

X-ray fluorescence (XRF) has become a key non-destructive technique for the analysis of fragile or immovable artworks, such as paintings and sculptures, where invasive methods are not viable (Liss & Stout, 2017; Marguí et al., 2022; Osman, 2020). Its portability allows for in situ investigations in museums and archaeological sites, combining the preservation of cultural heritage with efficient data acquisition (Ferretti & Tirello, 2009; Franzi et al., 2024; Wang et al., 2022). Moreover, XRF's capability to detect trace elements supports the study of historical production processes, restoration interventions, material degradation, and pigment provenance (Andrić et al., 2021; Franzi et al., 2024), establishing it as an essential tool in cultural heritage research (Felix & Pereira, 2021).

Despite these strengths, XRF's analytical performance is affected by the heterogeneity of the material matrix. While homogeneous samples enable accurate quantification, layered or composite objects, such as multilayered paintings, limit the technique to qualitative or semi-quantitative interpretations due to compositional variability (Andrić et al., 2021; Felix & Pereira, 2021; Sitko & Zawisza, 2012). In the analysis of historical painted surfaces, XRF identifies elements associated with specific pigments, while trace elements can provide insights into the geographic origin of raw materials (Calza, 2013; Moioli & Seccaroni, 2000). However, spectral artifacts originating from the instrument itself can undermine the accuracy of results, especially when they coincide with elemental markers critical for provenance analysis (Gallhofer & Lottermoser, 2018; Laperche & Lemière, 2020).

This study investigates the origin and impact of spectral artifacts in the Bruker Tracer III portable spectrometer, an instrument widely employed in archaeometric research. Reference samples from the Nuclear Instrumentation Laboratory (UFRJ/Coppe/LIN) and the sculpture *Head of Apollo* from the Eva Klabin House Museum in Rio de Janeiro were analyzed. The sculpture, carved from marble ($34.0 \times 27.0 \times 28.0$ cm), is attributed to Greece and dates between the 3rd and 1st centuries BCE. It represents the head of a statue identified as Apollo, the deity associated with the sun, music, and reason. Greek marble sculptures were often polychrome and frequently integrated into architectural elements of temples. A fitting at the top of the skull suggests that this piece may have served as a support for a cornice or entablature (Casa Museu Eva Klabin, 2024).

The marble used in the sculpture is a metamorphic rock composed primarily of calcite ($\mathrm{CaCO_3}$) or dolomite ($\mathrm{CaMg(CO_3)_2}$). It often contains trace elements and impurities that can aid in determining the quarry of origin. However, the compositional similarity between different marble sources necessitates the application of complementary analytical techniques for reliable provenance determination (Celik & Sert, 2020; Vaggelli et al., 2014).

In this context, XRF analysis was conducted on the Head of Apollo sculpture with two primary objectives:

(i) identify any traces of polychromy on the surface;

(ii) detect trace elements that could provide insights into the probable geographic origin of the marble.

The analysis was qualitative and exploratory, representing an initial survey designed to inform and support future, more comprehensive studies on the composition and provenance of the piece.

Material and methods

Thirteen reference samples, consisting of pure elements and compounds, were analyzed under two experimental conditions: with and without the radiation safety cap. Four of these samples were measured in both configurations to enable direct comparison. All measurements were carried out using the portable Tracer III XRF spectrometer (Bruker), operating at 40 kV and 35 μA, with an acquisition time of 60 seconds per spectrum. Data was processed using *ARTAX* (Bruker) and *OriginPro* 8.5 software. Figure 1 illustrates the experimental setup, including the measurement points on the *Head of Apollo* sculpture.

Figure 1(a) shows the setup used for measurements without the safety cap. In this configuration, pressed pellets were placed on a sample table positioned at the instrument's nose, providing a stable surface for analysis.

The sample table, visible in Figure 1(a) as a hexagonal accessory, was used to support the samples during acquisition. The distance between the X-ray window, located at the tip of the instrument's nose, and the pellet surface was approximately 7.0 mm.

Figure 1 - Experimental setups with the Tracer III spectrometer: (a) measurement without the radiation safety cap, (b) measurement with the radiation safety cap, (c) analyzed points on the sculpture, (d) front view of the *Head of Apollo* sculpture.

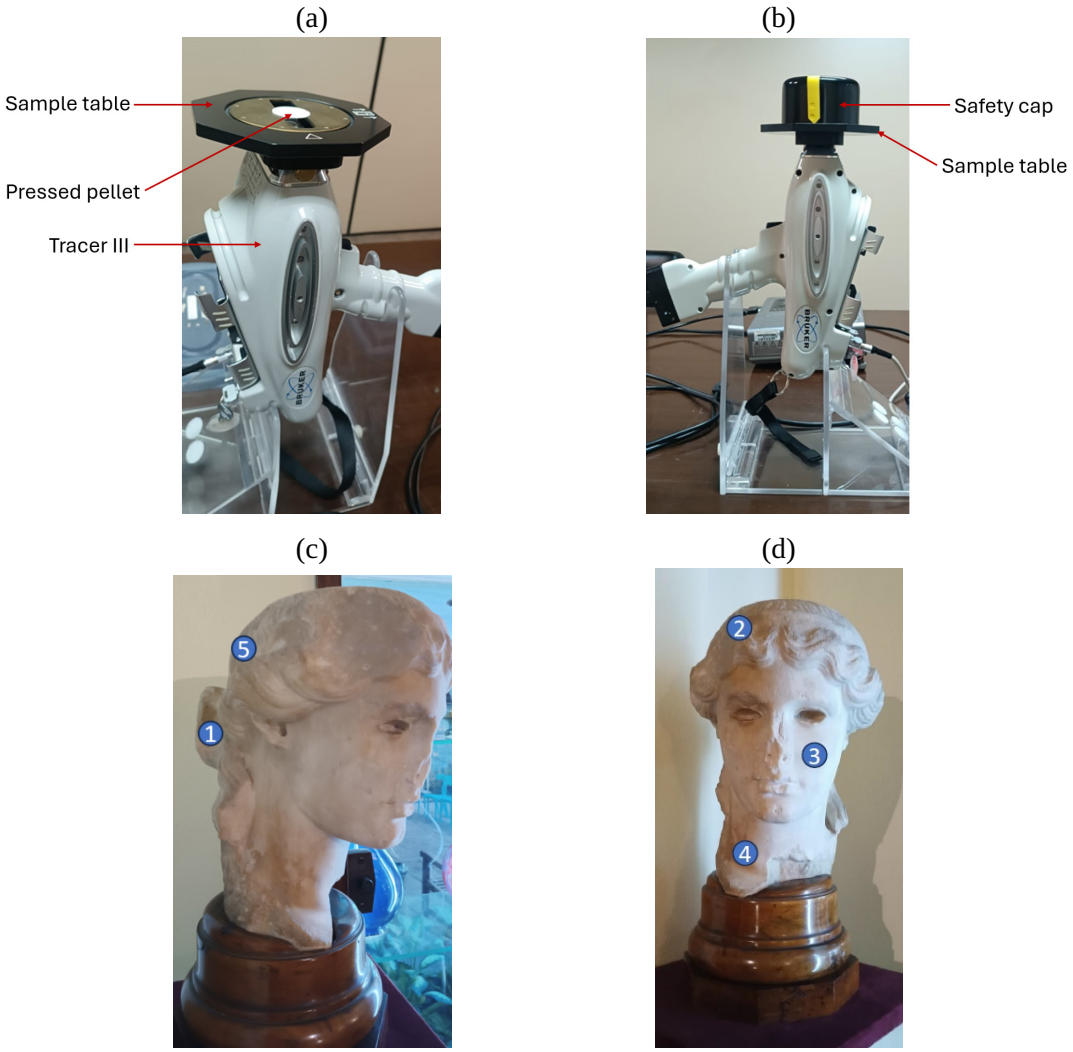

All pellet measurements were conducted using this same configuration, thereby maintaining a consistent distance between the X-ray window and the sample throughout the experiment. It is important to note that, for safety reasons, the instrument does not operate unless an object is placed in front of the X-ray window.

Figure 1(b) depicts the configuration with the safety cap in place. The safety cap is a black, hollow cylindrical accessory with a diameter of 8.0 cm and a height of 5.0 cm, featuring one open face that fits over the sample table. In this arrangement, the instrument can operate even without a sample. The spectrum of the safety cap itself was acquired using this setup, in the absence of any sample. For pellet measurements with the safety cap, the samples were positioned on the sample table, and the safety cap was fitted over them, maintaining the setup identical to that shown in Figure 1(b). Figures 1(c) and 1(d) indicate the locations selected for XRF analysis on the *Head of Apollo* sculpture.

Figure 2 presents the accessories of the portable instrument used in the experiment, the sample table and the safety cap, with selected dimensions indicated.

The samples, prepared as pressed pellets at the Nuclear Instrumentation Laboratory (LIN/UFRJ), have an average diameter of 25.5 mm and an average thickness of 0.7 mm and contain the following elements/compounds:

- **Pure elements:** cobalt (Co), tungsten (W), and antimony (Sb);
- **Compounds:** dysprosium oxide (Dy_2O_3), gadolinium oxide (Gd_2O_3), manganese (III) oxide (Mn_2O_3), neodymium oxide (Nd_2O_3), praseodymium oxide (Pr_6O_{11}), samarium oxide (Sm_2O_3), titanium dioxide (TiO_2), potassium sulfate (K_2SO_4), rubidium nitrate ($RbNO_3$), ytterbium oxide (Yb_2O_3), and zirconium oxide (ZrO_2).

Figure 2 - Tracer III accessories used in the experiment: the sample table is shown on the left and the safety cap on the right.

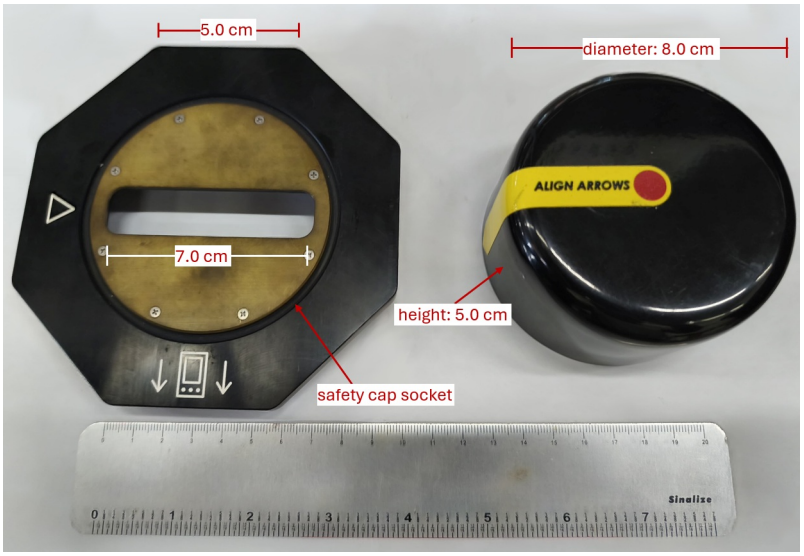

Boric acid was used as the binder in the pellet preparation. The pellets were pressed using a Schwing Siwa hydraulic press, applying a pressure of 12 tons for 15 minutes. Table 1 details the experimental measurement conditions for each pellet, specifying whether the safety cap was used, as well as identifying the pellets analyzed under both configurations, and also shows the compound or element name of each sample, total compound mass (Comp.), elemental mass fraction, elemental mass (M Elem.), final mass of the pellet (M Final), elemental concentration by weight (W%), and surface density (σ) in g/cm^2.

Table 1 - Pellets and their characteristics used for calibration.

Z	Pellet comp/elem.	Comp. (g)	Mass fraction	M Elem. (g)	M Final (g)	W (%)	σ (g/cm^2)
19	K_2SO_4	0.1004	0.4487	0.0451	0.528	8.53	0.10424
25	Mn_2O_3	0.0497	0.6960	0.0346	0.473	7.31	0.09339
27	Co	0.0510	1.0000	0.0510	0.476	10.71	0.09398
37	$RbNO_3$	0.0501	0.5796	0.0290	0.476	6.10	0.09394
40	ZrO_2	0.0097	0.7403	0.0072	0.471	1.53	0.09293
51	Sb	0.0502	1.0000	0.0502	0.520	9.60	0.1030
59	Pr_6O_{11}	0.0503	0.8277	0.0416	0.510	8.10	0.1010
60	Nd_2O_3	0.0507	0.8574	0.0435	0.530	8.20	0.1050
62	Sm_2O_3	0.0504	0.8624	0.0435	0.510	8.50	0.1010
64	Gd_2O_3	0.0508	0.8676	0.0441	0.510	8.70	0.1000
66	Dy_2O_3	0.0505	0.8713	0.0440	0.500	8.80	0.0982
70	Yb_2O_3	0.0492	0.8782	0.0432	0.470	9.20	0.0925
74	W	0.0501	1.0000	0.0501	0.510	9.80	0.1000

Spectral overlaps were observed in some cases between peaks originating from compounds or elements present in the pellets and artifact peaks. Notable examples include the Fe Kα1 line overlapping with the Dy Lα1 line, and the Ca Kα1 line overlapping with the Sb Lα1 line (Xrayweb, 2025). In both instances, the energy difference between these lines is smaller than the energy resolution of the spectrometer's semiconductor detector, making it impossible to adequately separate real peaks from instrumental artifacts, which can compromise spectral interpretation (Van Grieken & Markowicz, 2001). Additional cases of spectral overlap are detailed in the results section.

To evaluate the effect of the safety cap on the measurements, each reference sample was analyzed under different configurations: with the safety cap, without it, or in both conditions. Table 2 summarizes the experimental conditions applied to each compound or element during the measurements.

Table 2 - Experimental conditions used for each pressed reference pellet, indicating whether measurements were performed with, without, or in both safety cap configurations.

Pellet compound/element	Experimental condition
K_2SO_4	measured with the safety cap
Mn_2O_3	measured without the safety cap
Co	measured in both configurations
$RbNO_3$	measured in both configurations
ZrO_2	measured with the safety cap
Sb	measured in both configurations
Pr_6O_{11}	measured with the safety cap
Nd_2O_3	measured with the safety cap
Sm_2O_3	measured in both configurations
Gd_2O_3	measured with the safety cap
Dy_2O_3	measured with the safety cap
Yb_2O_3	measured with the safety cap
W	measured without the safety cap

The marble sculpture *Head of Apollo* was analyzed at five strategically chosen points, three on the hair, one on the face, and one on the neck, with the goal of maximizing the potential detection of pigment residues. Details can be seen in Figures 1(c) and 1(d).

Although no visible pictorial layers were observed, the possibility of surface traces could not be ruled out, thereby justifying the exploratory nature of the investigation.

The measurements were performed using the same acquisition parameters applied to the pressed pellets: 40 kV, 35 μA, and an acquisition time of 60 seconds per spectrum.

Results and Discussion

Reference samples

The analysis of the reference pellets allowed for the identification and characterization of artifact peaks generated by the Tracer III portable XRF spectrometer, distinguishing between interferences inherent to the instrument (Ti, Fe, Ni, Cu) and those associated with the radiation safety cap (Ca, Zn, Pb). The systematic approach involved acquiring spectra both with and without the safety cap, as well as analyzing the cap independently to determine its elemental composition.

Figures 3(a)–(f) show characteristic X-ray spectra of selected samples acquired with the safety cap, along with the spectrum of the cap alone, highlighting the impact of instrumental interferences on data interpretation. All spectra displayed peaks from Rh (the X-ray tube anode) and Ar (ambient atmosphere).

Independent analysis of the safety cap revealed the presence of Ca, Ti, Fe, Ni, Cu, Zn, and Pb, which were subsequently confirmed through comparison with reference samples of known composition, Table 3.

The results obtained from the analysis of reference pellets without the protective safety cap are presented in Table 4.

Peaks corresponding to Ca, Zn, and Pb disappeared when the safety cap was removed, confirming their origin in the cap's material. In contrast, Ti, Fe, Ni, and Cu peaks remained present under all measurement conditions, identifying them as intrinsic artifacts of the Tracer III instrument. It is important to note that, due to the limited thickness of the pellets (0.7 mm), the incident X-ray beam is partially attenuated, allowing it to reach the safety cap and generate interfering signals. In the case of infinitely thick samples (a few centimeters), this effect would be significantly reduced or even eliminated, as the beam would no longer reach the safety cap.

Figure 4 illustrate different responses of elemental peaks to the presence or absence of the safety cap, comparing the spectra obtained from the $RbNO_3$ and Co pellets, with and without the cap. In contrast, Figure 3 summarizes the cap's influence on peak generation. These findings emphasize the importance of applying preliminary corrections to avoid false positives in qualitative analyses.

Figure 3 - Characteristic X-ray spectra of selected samples measured with the safety cap compared to the spectrum of the radiation safety cap: (a) gadolinium oxide pellet, (b) potassium sulfate pellet, (c) neodymium oxide pellet, (d) rubidium nitrate pellet, (e) zirconium pellet, and (f) praseodymium oxide pellet.

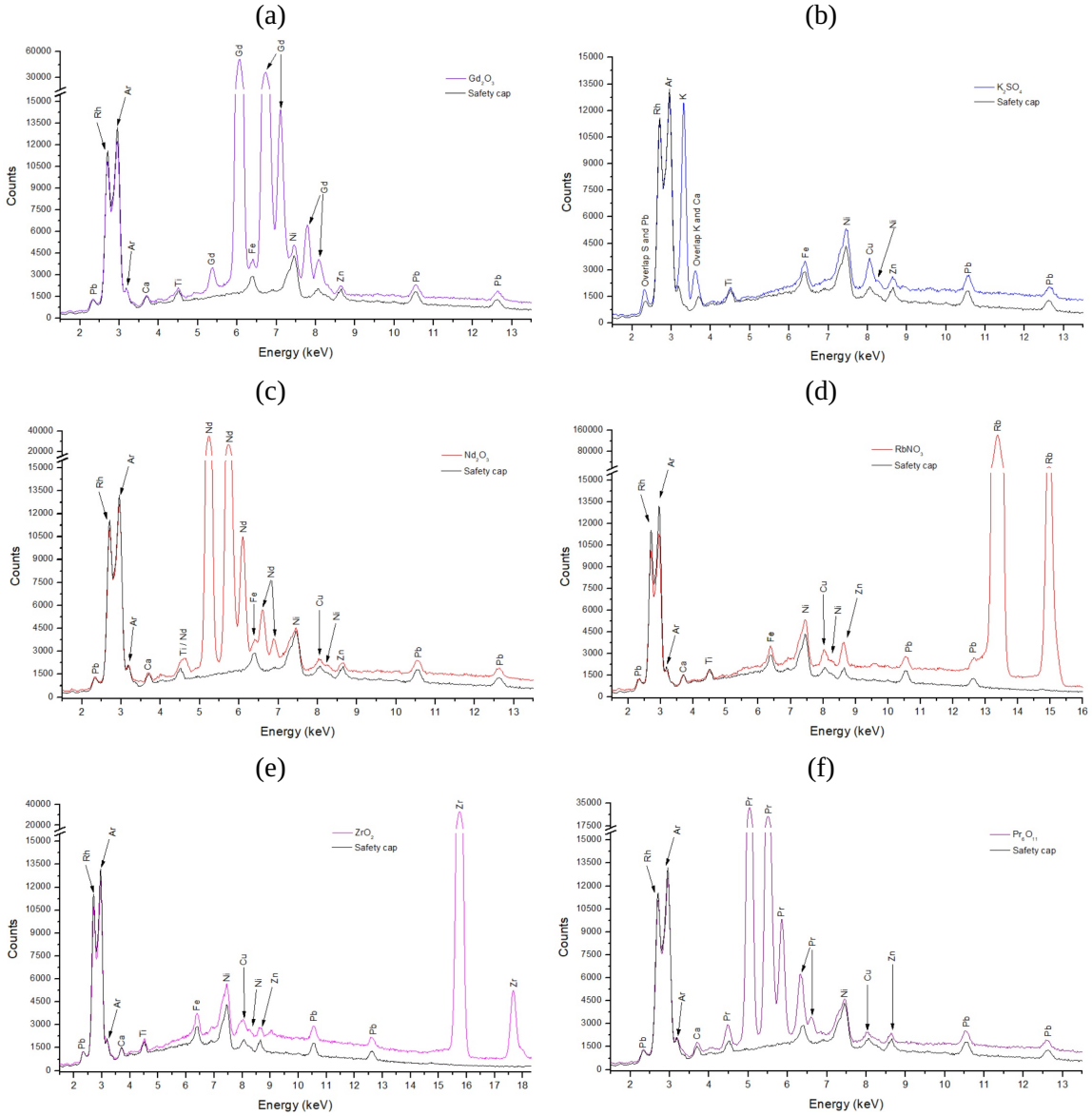

Figure 4 - Characteristic X-ray spectra samples measured with and without the protective safety cap: (a) cobalt pellet and (b) rubidium nitrate pellet

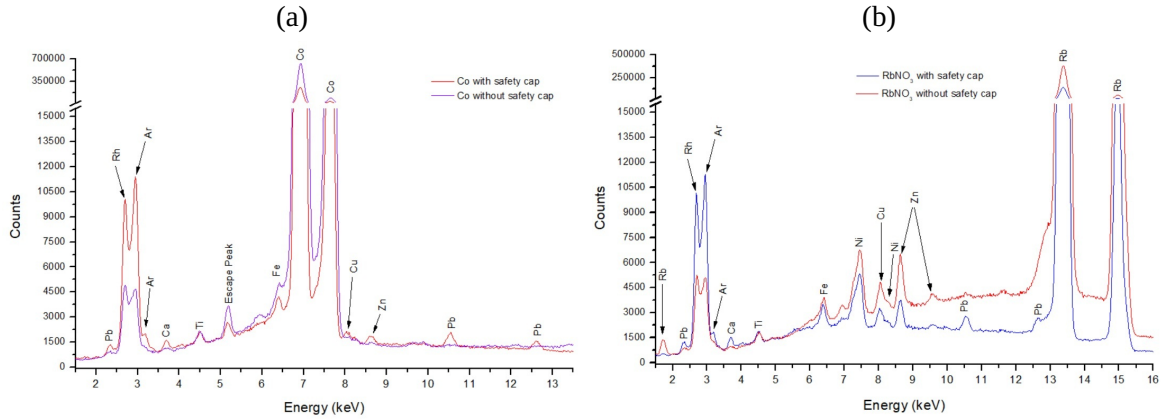

Table 3 - Analysis of reference pellets measured using the radiation safety cap using the Bruker Tracer III portable XRF spectrometer.

Compounds	Detected Elements	Remarks
Safety Cap	Ca, Ti, Fe, Ni, Cu, Zn, Pb	The elements Ca, Ti, Fe, Ni, Cu, Zn, and Pb are potential candidates for instrumental artifact peaks.
Co	Ca, Ti, Fe, Co, Cu, Zn, Pb	Overlap between Co Kβ_1 line and Ni Kα_1 line.
Dy_2O_3	Ca, Ti, Dy, Cu, Pb	Overlap between Dy Lα_1 line and Fe Kα_1 line; Dy Lβ_1 line and Ni Kα_1 line; and Dy Lγ_2 line and Zn Kα_1 line.
Gd_2O_3	Ca, Ti, Gd, Fe, Ni, Zn, Pb	Overlap between Gd Lγ_2 line and Cu Kα_1 line.
K_2SO_4	S, K, Ti, Fe, Ni, Cu, Zn, Pb	Overlap between K Kβ_1 line and Ca Kα_1 line.
Nd_2O_3	Ca, Ti, Nd, Fe, Ni, Cu, Zn, Pb	Overlap between Nd Lℓ line and Ti Kα_1 line.
Pr_6O_{11}	Ca, Pr, Ni, Cu, Zn, Pb	Overlap between Pr Lℓ line and Ti Kα_1 line; Pr Lγ_1 line and Fe Kα_1 line.
$RbNO_3$	Ca, Ti, Fe, Ni, Cu, Zn, Pb, Rb	No overlaps. Sample is suitable for identifying all artifact peaks within a single spectrum. However, the analysis suggests Zn contamination in the sample.
Sb	Ca, Ti, Fe, Ni, Cu, Zn, Pb	Overlap is observed between the Sb Lα_1 line and the Ca Kα_1 line, as well as between the Sb Lγ_1 and Lγ_2 lines and the Ti Kα_1 line.
Sm_2O_3	Ca, Ti, Sm, Cu, Zn, Pb	Overlap between Sm Lβ_1 line and Fe Kα_1 line; Sm Lγ_2 line and Ni Kα_1 line.
Yb_2O_3	Ca, Ti, Yb, Cu, Pb	Overlap is observed between the Yb Lℓ and Fe Kα_1 lines, Yb Lα_1 and Ni Kα_1 lines, and Yb Lβ_2 and Lβ_3 lines with the Zn Kα_1 line.
ZrO_2	Ca, Ti, Fe, Ni, Cu, Zn, Pb, Zr	Sample allows visualization of all instrumental and radiation safety cap artifact peaks.

Table 4 - Analysis of reference pellets measured without the protective safety cap using the Bruker Tracer III portable XRF spectrometer.

Compounds	Detected Elements	Remarks
Co	Ti, Fe, Co	The absence of Ca, Zn, and Pb peaks confirms that these elements originate exclusively from the composition of the safety cap.
Mn_2O_3	Ca, Ti, Mn, Ni, Cu, Zn	The presence of Zn and traces of Ca in the sample suggests contamination of the pellet with these elements. Additionally, overlap occurs between the Mn Kβ_1 peak and the Fe Kα_1 line.
$RbNO_3$	Ti, Fe, Ni, Cu, Zn, Rb	Confirms Ca and Pb as artifacts from the safety cap.
Sb	Sb, Fe, Ni, Cu, Zn	Confirms Ca and Pb as artifacts from the safety cap. The presence of Zn suggests contamination of the antimony pellet with this element.
Sm_2O_3	Ti, Sm, Cu, Ni, Zn	Confirms Ca and Pb as artifacts from the safety cap. The presence of Zn suggests contamination of the antimony pellet with this element.
W	Ti, Fe, W, Bi	Confirms Ca and Pb as artifacts from the safety cap. Overlaps are observed between the following lines: W Lℓ with Ni Kα_1, W Lα_1 with Cu Kα_1, and W Lα_2 with Zn Kα_1. The analysis also suggests bismuth contamination in the sample.

A comparison of spectra acquired from samples measured with and without the safety cap, Figures 4(a) and 4(b), demonstrating significant variations in the counts of Rh and Ar peaks. These findings suggest that the safety cap induces scattering of radiation back toward the detector, thereby increasing the counts of these characteristic peaks. Additionally, the increase observed in the Ar peak may be attributed not only to direct excitation by the X-ray source but also to secondary excitation by characteristic radiation from lead. Since the characteristic energy of Pb is closer to the excitation energy of argon, Pb fluorescence may also probabilistically excite Ar atoms in the surrounding air along the return path to the detector, resulting in increased detection of Ar characteristic X-rays.

Head of Apollo

Following the identification and validation of artifact peaks generated by the XRF spectrometer in reference samples, the methodology was applied to analyze the *Head of Apollo* sculpture, incorporating corrections for the effects of these pre-characterized instrumental interferences.

The elemental analysis of the sculpture detected S, Ca, Ti, Mn, Fe, Cu, Zn, Pb and Sr, see Figure 5. The prominent calcium peak aligns with the carbonate composition of marble, while Mn, Fe, and Sr correspond to trace elements typically associated with distinct quarries. To accurately infer the material's provenance, quantitative analyses are essential, as they would clarify whether the detected concentrations originate from ancient pigments, restoration patinas, or the geological matrix (Magrini et al., 2018).

Figure 5 - Overlaid spectra from the five measurement points on the marble sculpture *Head of Apollo*.

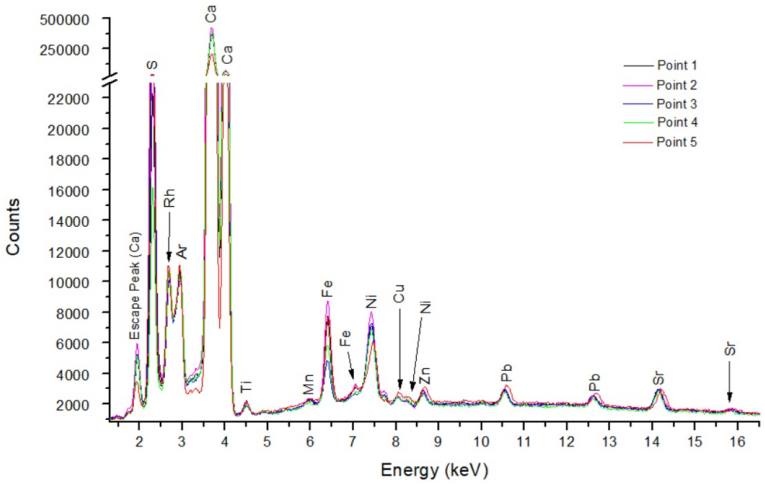

The presence of Si and K may further contribute to determining the marble composition used in the Apollo sculpture. Additional chemical components, such as FeO, Fe_2O_3, Al_2O_3, SiO_2, K_2O, and Na_2O, may occur in low concentrations and influence the marble's mineralogy (Celik & Sert, 2020). Elements like Ti, Zn, and Pb are also consistent with trace signatures of marbles sourced from quarries supplying the Mediterranean during antiquity (Poretti et al., 2017). In the case of the *Head of Apollo* measurements, conducted without the radiation protective safety cap, the detection of Zn and Pb confirms their intrinsic origin in the sculpture. However, the interpretation of Ti remains ambiguous: although cited in the literature as a potential trace element in marbles, it was identified as an intrinsic artifact peak of the equipment.

Elements such as Pb, Cu, Ni, and Zn may derive from sulfide or oxide inclusions, often present in marbles as submicroscopically distributed impurities with dimensions of a few micrometers (Poretti et al., 2017). This hypothesis explains the consistent detection of S across all spectra.

The interpretation of Ti, Cu and Ni, however, remains uncertain. While Ti is referenced as a trace element in marbles (Poretti et al., 2017), its low spectral intensity and similarity to instrumental artifacts complicates definitive attribution. Similarly, Cu and Ni, which also appears as equipment-derived interference, cannot be conclusively assigned to either natural or instrumental sources. In contrast Fe exhibited peak intensities exceeding those recorded in pellet measurements suggesting its probable presence either as residue from pictorial layers or as a naturally occurring trace element within the marble matrix.

Figure 6 presents a comparison between the X-ray spectrum acquired from measurement point 1, on the *Head of Apollo*, see Figure 1(c), and that of an $RbNO_3$ pellet measured without the safety cap.

Figure 6 - X-ray spectrum acquired from measurement point 1 on the *Head of Apollo*, compared with the spectrum of an $RbNO_3$ pellet measured without the safety cap.

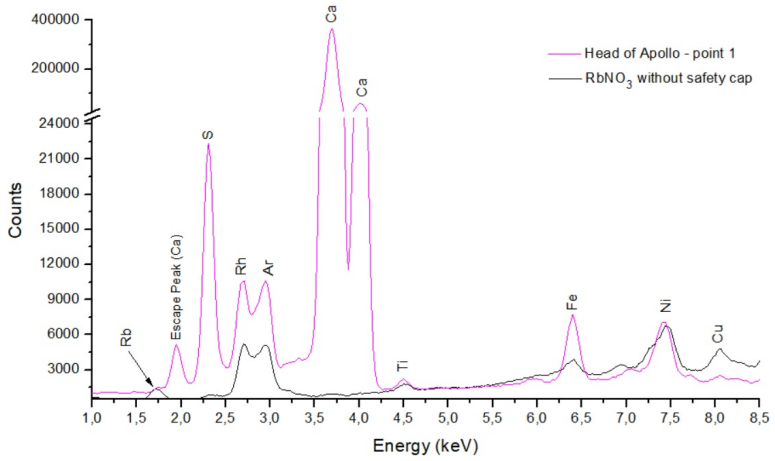

The experimental conditions for the sculpture and the pellet measurements, both conducted without the safety cap, are comparable. Based on this comparison, it is qualitatively evident that, although the Fe signal includes a contribution from the instrument itself, iron is indeed present in the analyzed area of the sculpture.

Conclusions

The results confirmed the generation of artifact peaks by the portable XRF Tracer III spectrometer, with Ti, Fe, Ni, and Cu identified as intrinsic equipment interferences, while Ca, Zn, and Pb were linked to the safety cap. Distinguishing these artifacts from the samples' true composition proved critical to avoiding misinterpretations, particularly in analyses of artworks and archaeological materials, where trace elements are pivotal for inferring provenance or identifying pigments.

In the application to the *Head of Apollo* sculpture, elements such as Ca, Fe, Mn, and Sr aligned with the marble's composition, whereas Zn and Pb suggested natural impurities or historical residues. However, the presence of Ti, Ni, and Cu as artifacts introduced ambiguities, necessitating spectral corrections to prevent data distortions. Qualitative analysis could not conclusively determine whether Zn and Pb originated from the geological matrix, pigments, or conservation interventions, underscoring the need for complementary methodologies.

While this study characterized the Tracer III's artifact peaks, unresolved gaps require further investigation. These include the determination of the instrument's sensitivity curve and limits of detection (LOD); the verification of detector linearity; the use of certified reference samples to refine analytical accuracy; the comparison of data with spectra from different pXRF spectrometer models to assess equipment-specific biases; the validation of reproducibility across multiple units of the same equipment to confirm intrinsic variations and the implementation of quantitative analyses to measure the relative contribution of artifacts in *in situ* measurements.

For the *Head of Apollo*, integrating XRF with techniques such as X-ray diffraction (XRD) and Raman spectroscopy could resolve spectral overlaps and corroborate hypotheses regarding marble provenance or pigment residues. Finally, identifying these instrumental interferences optimizes XRF spectral interpretation in archaeometry, ensuring higher precision in assessing the chemical composition of historical objects.

Acknowledgments

This study was supported by the Conselho Nacional de Desenvolvimento Científico e Tecnológico (CNPq), INCT INAIS (grant 406303/2022-3), and was partially funded by the Coordenação de Aperfeiçoamento de Pessoal de Nível Superior (CAPES) – Finance Code 001. The authors would also like to thank the Fundação de Amparo à Pesquisa do Estado do Rio de Janeiro (FAPERJ) for their financial support.

Author Contributions

R. M. de P. S. Borges participated in: conceptualization, data curation, formal analysis, investigation, methodology, visualization, and writing – original draft. **J. E. Cavalcante**, **I. V. N. da S. Franzi**, and **A. G. de Paula** participated in: investigation. **E. Azevedo** and **R. T. Lopes** participated in: resources and funding. **D. F. Oliveira** participated in: validation, resources, supervision, and writing – review and editing.

Conflicts of Interest

The authors declare no conflict of interest.

References

Andrić, V., Gajić-Kvaščev, M., Crkvenjakov, D. K., Marić-Stojanović, M., & Gadžurić, S. (2021). Evaluation of pattern recognition techniques for the attribution of cultural heritage objects based on the qualitative XRF data. *Microchemical Journal*, *167*, 106267. https://doi.org/10.1016/j.microc.2021.106267

Calza, C. (2013). Análise científica de obras de arte e objetos de valor histórico-cultural. In W. Barja (Org.), *Gestão Museológica: questões teóricas e práticas* (pp. 97–108). Câmara dos Deputados. https://bd.camara.leg.br/bd/bitstream/handle/bdcamara/14257/gestao_museologica_questoes.pdf?sequence=5

Casa Museu Eva Klabin. (2024). *Head of Apollo*. http://evaklabin.provisorio.ws/visitavirtual/

Celik, M. Y., & Sert, M. (2020). The importance of “Pavonazzetto marble” (Docimium-Phrygia/Iscehisar-Turkey) since ancient times and its properties as a global heritage stone resource. *Environmental Earth Sciences*, *79*(9), 201. https://doi.org/10.1007/s12665-020-08943-2

Felix, V. S., & Pereira, M. O. (2021). Analysis of painting Victor Meirelles’ “Passagem de Humaitá” by XRF. *Brazilian Journal of Radiation Sciences*, *9*(1A), 1–10. https://doi.org/10.15392/bjrs.v9i1A.1371

Ferretti, M., & Tirello, R. A. (2009). Princípios e aplicações de espectroscopia de fluorescência de Raios X (FRX) com instrumentação portátil para estudo de bens culturais. *Revista CPC*, (7), 74–98. https://doi.org/10.11606/issn.1980-4466.v0i7p74-98

Franzi, I. V. N. D. S., Paula, A. G. D., Cavalcante, J. E., Borges, R. M. D. P. S., Gomes, R. A. F., Oliveira, D. F. D., & Lopes, R. T. (2024). On-Site X-Ray Fluorescence Analysis of Sculptures of the Archdiocesan Museum of Sacred Art of Rio de Janeiro’s Collection. *X-Ray Spectrometry*, *54*(4), 366–377. https://doi.org/10.1002/xrs.3467

Gallhofer, D., & Lottermoser, B. G. (2018). The influence of spectral interferences on critical element determination with portable X-ray fluorescence (pXRF). *Minerals*, *8*(8), 320. https://doi.org/10.3390/min8080320

Laperche, V., & Lemière, B. (2020). Possible pitfalls in the analysis of minerals and loose materials by portable XRF, and how to overcome them. *Minerals*, *11*(1), 33. https://doi.org/10.3390/min11010033

Liss, B., & Stout, S. (2017). Materials characterization for cultural heritage: XRF case studies in archaeology and art. In M. Vincent, V. López-Menchero Bendicho, M. Ioannides, & T. Levy (Eds.), *Heritage and Archaeology in the Digital Age* (pp. 49–65). Springer. https://doi.org/10.1007/978-3-319-65370-9_3

Magrini, D., Attanasio, D., Bracci, S., Cantisani, E., & Prochaska, W. (2018). Innovative application of portable X-ray fluorescence (XRF) to identify Göktepe white marble artifacts. *Archaeological and Anthropological Sciences*, *10*, 1141–1152. https://doi.org/10.1007/s12520-016-0444-7

Marguí, E., Queralt, I., & de Almeida, E. (2022). X-ray fluorescence spectrometry for environmental analysis: Basic principles, instrumentation, applications and recent trends. *Chemosphere*, *303*(1), 135006. https://doi.org/10.1016/j.chemosphere.2022.135006

Moioli, P., & Seccaroni, C. (2000). Analysis of art objects using a portable X-ray fluorescence spectrometer. *X-Ray Spectrometry: An International Journal*, *29*(1), 48–52. https://doi.org/10.1002/(SICI)1097-4539(200001/02)29:1<48::AID-XRS404>3.0.CO;2-H

Osman, E. (2020). Spectrometry as a non-destructive technique in identifying cultural archaeological heritage: Some case studies illustrating 'characterization without devastation'. In A. K. Shukla (Ed.), *Spectroscopic Techniques for Archaeological and Cultural Heritage Research* (2nd ed., pp. 1–9). IOP Publishing. https://doi.org/10.1088/978-0-7503-2616-2ch1

Poretti, G., Brilli, M., de Vito, C., Conte, A. M., Borghi, A., Günther, D., & Zanetti, A. (2017). New considerations on trace elements for quarry provenance investigation of ancient white marbles. *Journal of Cultural Heritage*, *28*, 16–26. https://doi.org/10.1016/j.culher.2017.04.008

Sitko, R., & Zawisza, B. (2012). Quantification in X-ray fluorescence spectrometry. In S. K. K. Sharma (Ed.), *X-ray spectroscopy* (pp. 137–162). IntechOpen. https://doi.org/10.5772/29367

Vaggelli, G., Serra, M., Cossio, R., & Borghi, A. (2014). A New Approach for Provenance Studies of Archaeological Finds: Inferences from Trace Elements in Carbonate Minerals of Alpine White Marbles by a Bench-to-Top μ-XRF Spectrometer. *International Journal of Mineralogy*, *2014*(1), 217916. https://doi.org/10.1155/2014/217916

Van Grieken, R., & Markowicz, A. (2001). *Handbook of X-ray Spectrometry*. CRC Press.

Wang, Z., Zhang, Z., Wang, F., & Liu, J. (2022). A pXRF-based approach to identifying the material source of stone cultural relics: a case study. *Minerals*, *12*(2), 199. https://doi.org/10.3390/min12020199

Xrayweb. (2025). *IXAS X-ray data for the elements*. https://xraydb.xrayabsorption.org/element/